PHYSICAL REVIEW C **72**, 031901(R) (2005)

Scaling of charged particle production in d+Au collisions at $\sqrt{s_{NN}} = 200$ GeV

B. B. Back,[1] M. D. Baker,[2] M. Ballintijn,[4] D. S. Barton,[2] B. Becker,[2] R. R. Betts,[6] A. A. Bickley,[7] R. Bindel,[7] W. Busza,[4] A. Carroll,[2] M. P. Decowski,[4] E. García,[6] T. Gburek,[3] N. George,[2] K. Gulbrandsen,[4] S. Gushue,[2] C. Halliwell,[6] J. Hamblen,[8] A. S. Harrington,[8] C. Henderson,[4] D. J. Hofman,[6] R. S. Hollis,[6] R. Hołyński,[3] B. Holzman,[2] A. Iordanova,[6] E. Johnson,[8] J. L. Kane,[4] N. Khan,[8] P. Kulinich,[4] C. M. Kuo,[5] J. W. Lee,[4] W. T. Lin,[5] S. Manly,[8] A. C. Mignerey,[7] R. Nouicer,[2,6] A. Olszewski,[3] R. Pak,[2] I. C. Park,[8] H. Pernegger,[4] C. Reed,[4] C. Roland,[4] G. Roland,[4] J. Sagerer,[6] P. Sarin,[4] I. Sedykh,[2] W. Skulski,[8] C. E. Smith,[6] P. Steinberg,[2] G. S. F. Stephans,[4] A. Sukhanov,[2] M. B. Tonjes,[7] A. Trzupek,[3] C. Vale,[4] G. J. van Nieuwenhuizen,[4] R. Verdier,[4] G. I. Veres,[4] F. L. H. Wolfs,[8] B. Wosiek,[3] K. Woźniak,[3] B. Wysłouch,[4] and J. Zhang[4]

[1]*Argonne National Laboratory, Argonne, Illinois 60439-4843, USA*
[2]*Brookhaven National Laboratory, Upton, New York 11973-5000, USA*
[3]*Institute of Nuclear Physics PAN, Kraków, Poland*
[4]*Massachusetts Institute of Technology, Cambridge, Massachusetts 02139-4307, USA*
[5]*National Central University, Chung-Li, Taiwan*
[6]*University of Illinois at Chicago, Chicago, Illinois 60607-7059, USA*
[7]*University of Maryland, College Park, Maryland 20742, USA*
[8]*University of Rochester, Rochester, New York 14627, USA*

(Received 30 September 2004; published 29 September 2005)

The measured pseudorapidity distributions of primary charged particles over a wide pseudorapidity range of $|\eta| \leqslant 5.4$ and integrated charged particle multiplicities in d+Au collisions at $\sqrt{s_{NN}} = 200$ GeV are presented as a function of collision centrality. The longitudinal features of d+Au collisions at $\sqrt{s_{NN}} = 200$ GeV are found to be very similar to those seen in p+A collisions at lower energies. The total multiplicity of charged particles is found to scale with the total number of participants according to $N_{\rm ch}^{d\rm Au} = \frac{1}{2}\langle N_{\rm part}\rangle N_{\rm ch}^{pp}$, and the energy dependence of the density of charged particles produced in the fragmentation region exhibits extended longitudinal scaling.

DOI: 10.1103/PhysRevC.72.031901 PACS number(s): 25.75.Dw, 25.75.Gz

Charged particle multiplicities have been studied extensively in high energy collisions because of the intrinsic interest in understanding the production mechanism. More recent interest comes in the context of searching for and studying new forms of matter that are expected to be created in heavy ion collisions at ultrarelativistic energies. A key quantity that contains information about the longitudinal aspects of the multiparticle production process and has provided valuable input for discriminating between phenomenological models in the past [1] is the rapidity distribution of identified particles. When particle identification is not available, the almost equivalent pseudorapidity distribution of charged particles suffices. For this reason, such distributions have been studied in detail in hadron+proton [2], hadron+nucleus [3,4], and nucleus+nucleus [5] collisions.

Since the first collisions were achieved at the BNL Relativistic Heavy Ion Collider (RHIC), the PHOBOS Collaboration has obtained extensive information on pseudorapidity distributions of charged particles produced in Au+Au collisions for energies $\sqrt{s_{NN}}$ between 19.6 and 200 GeV and over a large range of collision geometries. We have observed, for example, that the particle density in the midrapidity region changes smoothly as a function of $\sqrt{s_{NN}}$ [6] and that the total charged particle production scales linearly with the number of participants [7]. Further detailed observations of the shape of the pseudorapidity distribution show a scaling according to the "limiting fragmentation" hypothesis [8].

The study of a simpler system such as d+Au at the same energy as Au+Au is essential to gain insight into which aspects of the data follow from the initial interacting states or general properties of the hadronic production process, and which are the consequence of the very different environments created in d+Au and Au+Au collisions.

In this Rapid Communication, we present the results of detailed measurements of the pseudorapidity distributions of primary charged particles, $dN_{\rm ch}/d\eta$, as a function of collision centrality in d+Au collisions at $\sqrt{s_{NN}} = 200$ GeV over a wide pseudorapidity range of $|\eta| \leqslant 5.4$. The results for d+Au collisions are compared to Au+Au collisions and inelastic $p(\bar{p})$+p collisions at $\sqrt{s_{NN}} = 200$ GeV as well as to $p(\pi^+, \mathrm{K}^+)$+nucleus collisions at lower energies. To continue our previous studies presented in Ref. [9], to see to what extent the simple concept of the "wounded nucleon model" [10] continues to apply at higher energies, and to search for evidence of the onset of gluon saturation, the results of d+Au collisions are compared with several recent calculations [11] and predictions [12]. Within systematic uncertainties, the data can be described by the parton saturation model, while the AMPT model fails to reproduce the data in peripheral d+Au collisions.

The data were obtained with the multiplicity array of the PHOBOS detector [13]. The array consists of an octagonal barrel of silicon detectors, the Octagon, surrounding the interaction region in an approximately cylindrical geometry covering $|\eta| \leqslant 3.2$. This array is augmented by two sets of three annular silicon counter arrays, the Rings, along the beam pipe far forward and backward of the interaction region ($3.0 < |\eta| < 5.4$). This array is identical to that used in our

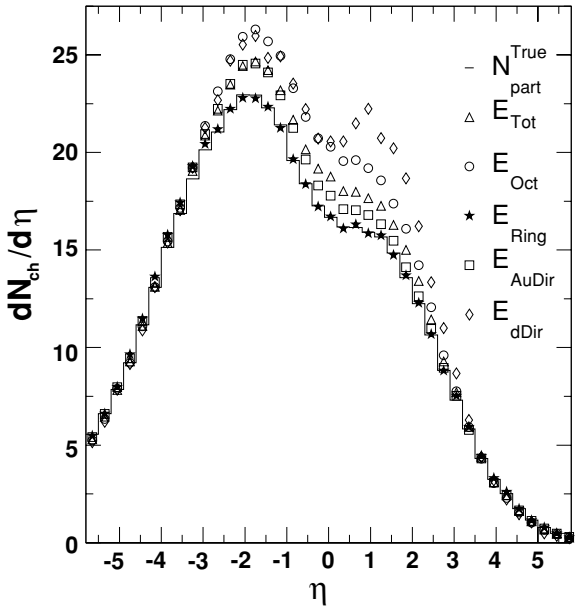

FIG. 1. HIJING simulations of the $dN_{\rm ch}/d\eta$ distributions of charged particles in d+Au collisions at $\sqrt{s_{NN}} = 200$ GeV obtained for a selected $N_{\rm part}^{\rm True} = 15$ (solid line) compared with four other distinct centrality measures (symbols) done for centrality bins that yield to the same $\langle N_{\rm part}^{\rm True}\rangle$.

study of Au+Au collisions [8]. The setup also includes two sets of 16 scintillator counters ($3.0 < |\eta| < 4.5$) which were used in the primary event trigger and in the offline event selection.

The centrality determination was based on the observed total energy deposited in the Ring counters, $E_{\rm Ring}$, which is proportional to the number of charged particles hitting these detectors. The choice of this centrality measure was based on extensive studies utilizing both data and Monte Carlo (MC) simulations to identify a measure which showed minimum effects of auto-correlations on the final $dN_{\rm ch}/d\eta$ result. We studied four other distinct centrality measures based on the multiplicity in different regions of pseudorapidity, called $E_{\rm Tot}$, $E_{\rm Oct}$, $E_{\rm AuDir}$, and $E_{d\rm Dir}$, discussed previously in Ref. [9]. Using MC simulations, we found that these other centrality measures, which are obtained over limited regions of pseudorapidity, all induce significant bias on the $dN_{\rm ch}/d\eta$ distribution, as shown in Fig. 1. These effects can be large, resulting in enhancements (suppressions) in the reconstructed midrapidity yields of up to ∼30% for central (peripheral) collisions. The MC simulations used in the study included both HIJING [14] and AMPT [15] event generators coupled to a full GEANT [16] simulation of the PHOBOS detector. To obtain $dN_{\rm ch}/d\eta$, the BRAHMS collaboration [17] recently used a centrality measure similar to $E_{\rm Oct}$. According to our analysis, $E_{\rm Oct}$ (and therefore the BRAHMS method) shows undesirable biases arising from auto-correlations.

Ratios of the reconstructed $dN_{\rm ch}/d\eta$ distributions obtained from the five centrality measures for data and, independently, for the MC simulations were found to agree, giving confidence in the entire methodology. Knowledge of the unbiased MC simulated "truth" distributions then provided a clear choice of the optimum centrality measure based on the Ring detectors, which resulted in the least bias on the measurements.

TABLE I. Estimated number of nucleon participants in the incoming gold $\langle N_{\rm part}^{\rm Au}\rangle$ and deuteron $\langle N_{\rm part}^{d}\rangle$ nuclei ($\langle N_{\rm part}\rangle = \langle N_{\rm part}^{d}\rangle + \langle N_{\rm part}^{\rm Au}\rangle$) and the number of collisions $\langle N_{\rm coll}\rangle$ as a function of centrality in d+Au collisions. The integrated charged particle multiplicity in the measured region and the estimated total charged particle multiplicity extrapolated to the unmeasured region are listed. All errors are systematic (90% C.L.).

Cent. (%)	$\langle N_{\rm part}^{\rm Au}\rangle$	$\langle N_{\rm part}^{d}\rangle$	$\langle N_{\rm coll}\rangle$	$N^{\rm ch}_{\lvert\eta\rvert\leqslant 5.4}$	$N^{\rm ch}_{\rm Tot}$
0–20	13.5 ± 1.0	2.0 ± 0.1	14.7 ± 0.9	157 ± 10	167^{+14}_{-11}
20–40	8.9 ± 0.7	1.9 ± 0.1	9.8 ± 0.7	109 ± 7	115^{+10}_{-8}
40–60	5.4 ± 0.6	1.7 ± 0.2	5.9 ± 0.6	74 ± 5	77^{+7}_{-5}
60–80	2.9 ± 0.5	1.4 ± 0.2	3.1 ± 0.6	46 ± 3	48^{+3}_{-3}
80–100	1.6 ± 0.4	1.1 ± 0.2	1.7 ± 0.5	28 ± 3	29^{+3}_{-3}
Min-Bias	6.6 ± 0.5	1.7 ± 0.1	7.1 ± 0.5	82 ± 6	87^{+7}_{-6}
50–70	3.9 ± 0.6	1.6 ± 0.2	4.2 ± 0.6	59 ± 4	62^{+5}_{-4}

The multiplicity signals of $E_{\rm Ring}$ were divided into five centrality bins, where each bin contained 20% of the total cross section. The trigger and vertexing efficiency was determined for each bin. Knowledge of the efficiency as a function of multiplicity allowed for the correct centrality bin determination in data as well as the extraction of the corresponding efficiency-averaged number of participants. A comparison of the data and the MC simulations yielded an overall efficiency of ∼83%.

Results of the Glauber calculations implemented in the MC simulations were used to estimate the average total number of nucleon participants $\langle N_{\rm part}\rangle$, the number of participants in the incident gold $\langle N_{\rm part}^{\rm Au}\rangle$, and the deuteron $\langle N_{\rm part}^{\rm d}\rangle$ nuclei, as well as the number of binary collisions $\langle N_{\rm coll}\rangle$ for each centrality bin (see Table I).

The details of the analysis leading to the measurements of $dN_{\rm ch}/d\eta$ can be found in Ref. [18]. The final results use the average of the two methods based on hit-counting and energy deposition. The measured $dN_{\rm ch}/d\eta$ was corrected for particles which were absorbed or produced in the surrounding material and for feed-down products from weak decays of neutral strange particles. Uncertainties in $dN_{\rm ch}/d\eta$ associated with these corrections range from 6% in the Octagon up to 28% in the Rings. These uncertainties dominate the systematic errors.

Figure 2 shows the $dN_{\rm ch}/d\eta$ distributions for d+Au collisions at $\sqrt{s_{NN}} = 200$ GeV in five centrality bins, 0–20% being the most central, and for minimum-bias events, discussed in detail in Ref. [9]. The pseudorapidity is measured in the nucleon-nucleon center-of-mass frame; a negative pseudorapidity corresponds to the gold nucleus direction. For the most central collisions, the mean η of the distribution is found to be negative, reflecting the net longitudinal momentum of the participants in the laboratory (NN) frame. For more peripheral collisions, the mean η tends to zero as the distribution becomes more symmetric. For measurements of d+Au in the nucleon-nucleon center-of-mass system, the Jacobian associated with

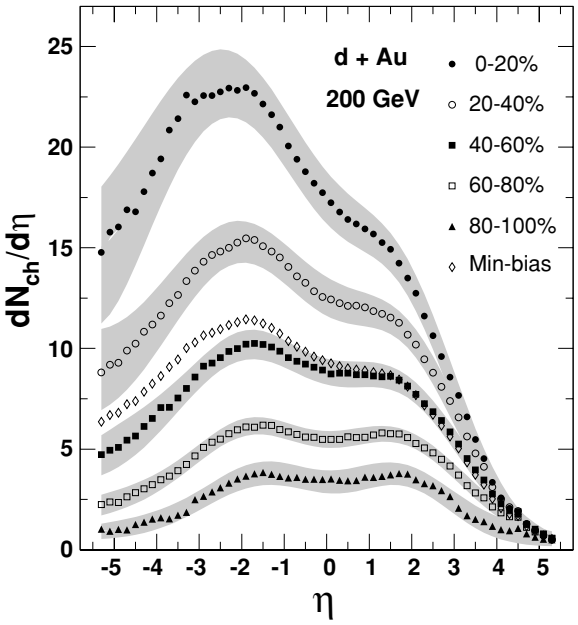

FIG. 2. Measured pseudorapidity distributions of primary charged particles from d+Au collisions at $\sqrt{s_{NN}} = 200\,\text{GeV}$ as a function of collision centrality. Shaded bands represent 90% confidence level systematic errors, and the statistical errors are negligible. The minimum-bias distribution is shown as open diamonds [9].

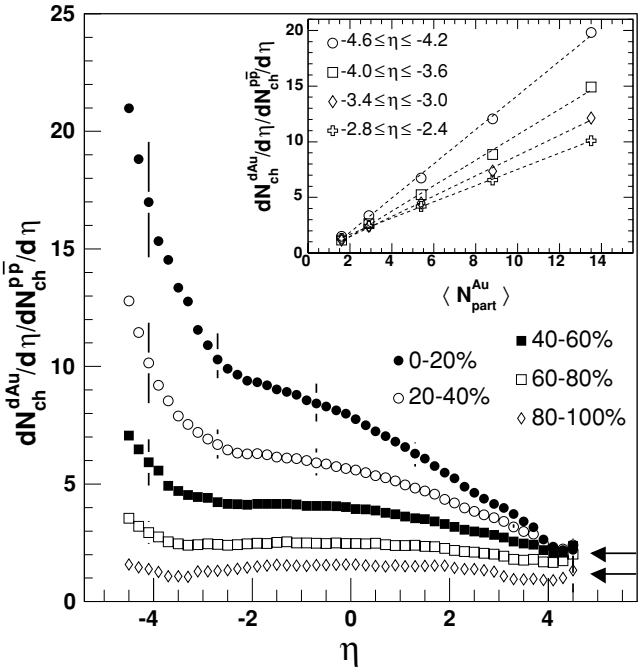

FIG. 3. Centrality dependence of the $dN_{\text{ch}}/d\eta$ ratio of d+Au collisions relative to the fit to the inelastic UA5 $p(\bar{p})$+p data [19] at the same energy. Arrows represent the $\langle N^{d}_{\text{part}}\rangle$ of the most central and most peripheral collisions. Typical systematic errors are shown for selected points. The inset figure shows the variation of the ratio as a function of $\langle N^{\text{Au}}_{\text{part}}\rangle$, for four η regions in the gold direction. Dashed lines represent a linear fit to the data.

the transformation dN_{ch}/dy and $dN_{\text{ch}}/d\eta$ naturally produces the "double-hump" structure in $dN_{\text{ch}}/d\eta$ even if there is no structure in dN_{ch}/dy. As a function of collision centrality, the integrated charged particle multiplicity in the measured region ($|\eta| \leqslant 5.4$) and the estimated total charged particle multiplicity extrapolated to the unmeasured region using guidance from the shifted p+nucleus data (see Fig. 6) are presented in Table I.

Now, we compare our d+Au results with $p(\bar{p})$+p and $p+A$ data obtained at lower energy and discuss the energy and centrality dependence of the data (see Fig. 3). The results are consistent with a picture in which the production of particles with rapidity near that of the incident deuteron (gold) is approximately proportional to the number of deuteron (gold) participants. These trends are consistent with lower energy $p+A$ data [20,21] and with the quark-parton model of Brodsky *et al.* [22].

Figure 4(a) shows that the total charged particle multiplicity scales linearly with $\langle N_{\text{part}}\rangle$ in both d+Au and Au+Au collisions. It also indicates that the transition between inelastic $p(\bar{p})$+p collisions and Au+Au collisions is not controlled simply by the number of participants, as even very central d+Au multiplicity per participant pair shows no signs of extrapolating to the Au+Au results. Not only do we find that the total charged particle production in d+Au scales linearly with $\langle N_{\text{part}}\rangle$, but also that the scaling relative to the $p(\bar{p})$+p multiplicity is energy independent and the same in all hadron + nucleus collisions [3]. This is evident from Figure 4(b) where the ratio $R_A = N_{\text{ch}}/N^{pp}_{\text{ch}}$ is plotted as a function of $\langle N_{\text{part}}\rangle$ for a large variety of systems and energies. Here N_{ch} is the integrated total charged particle multiplicity for $d+A$, $p+A$ [20], and N^{pp}_{ch} is for $p(\bar{p})$+p. Note that the ν ($\nu = \langle N_{\text{coll}}\rangle/\langle N^{d}_{\text{part}}\rangle$) of central d+Au collisions is twice that of minimum-bias p+Pb collisions.

It is this scaling, observed for the first time by Busza *et al.* [25], which led to the wounded nucleon model [26]. Based on the recent calculation presented by Białas *et al.* in Ref. [10], we conclude that the wounded nucleon model not only describes the total multiplicity but also the complete pseudorapidity distributions. Kharzeev *et al.* [11] find, however, that the data can also be well reproduced within the parton saturation model. Figure 5 shows the comparison of our data with the recent calculations of parton saturation [11] and the predictions of AMPT [12].

Finally, Fig. 6 compares $dN_{\text{ch}}/d\eta$ distributions of d+Au to p + Emulsion (Em) collisions at five energies [4,27,28], in the effective rest frame of both the projectile "beam" (a) and target (b). For p+Em data, the $dN_{\text{ch}}/d\eta$ distributions represent the sum of shower and gray tracks. Note that η is measured in different reference frames for d+Au and p+Em. This means that compared to d+Au collisions, the p+Em pseudorapidity distributions are suppressed by the Jacobian for $\eta + y_{\text{target}} \sim 0$. The 50–70% centrality bin of d+Au collisions was selected in order to match as well as possible $N^{\text{Au}}_{\text{part}}/N^{d}_{\text{part}}$ to $N^{\text{Em}}_{\text{part}}/N^{p}_{\text{part}}$ where $\langle N_{\text{part}}(p\text{Em})\rangle = 3.4$. The relative normalization of the $dN_{\text{ch}}/d\eta$ for $d+$ Au and p+Em collisions requires a ratio of $\langle N_{\text{part}}(d\text{Au})\rangle/\langle N_{\text{part}}(\text{pEm})\rangle = 1.6$ (a multiplicative factor of 1/1.6 has been applied to the d+A data), such that the data correspond to the same number of nucleons interacting with the nucleus. A remarkably good

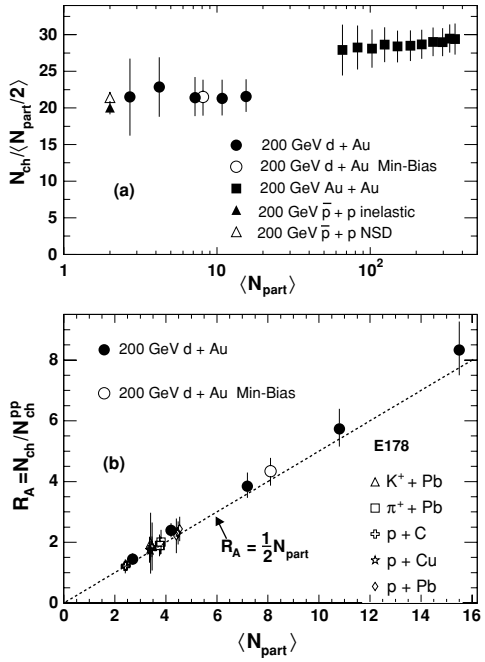

FIG. 4. (a) Total integrated charged particle multiplicity per participant pair in d+Au, Au+Au [7], $p(\bar{p})$+p inelastic [23] and $p(\bar{p})$+p nonsingle diffractive (NSD) [24] collisions at the same energy, $\sqrt{s_{NN}} = 200$ GeV. (b) Ratio $R_A = N_{\rm ch}/N_{\rm ch}^{pp}$, where $N_{\rm ch}^{pp}$ is the total number of charged particles for inelastic $p(\bar{p})$+p collisions, as a function of the total number of participant nucleons $\langle N_{\rm part}\rangle$ for different collision systems. The $\pi^+ + $ Pb, $p + $C, $p + $Cu, and p+Pb collisions are for $\sqrt{s_{NN}} = 19.4$, 13.8, and 9.8 GeV, and the $K^+ + $ Pb for $\sqrt{s_{NN}} = 13.8$, and 9.8 GeV from Ref. [20], respectively. For the d+Au and Au+Au data, the error bars indicate systematic errors (90% C.L.). Dashed line represents the linear relation $R_A = \frac{1}{2}\langle N_{\rm part}\rangle$.

agreement (extended longitudinal scaling) is observed in the fragmentation regions of the deuteron (gold) between d+A and p+Em collisions at different energies. Furthermore, the region in which charged particle densities are energy independent extend to lower $|\eta|$ with increasing collision energy in both

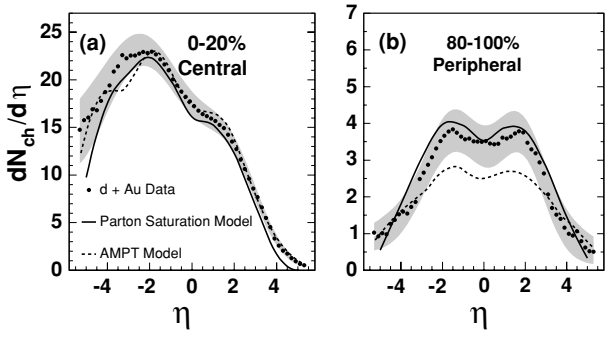

FIG. 5. (a) Comparison of pseudorapidity distributions from d+Au collisions at $\sqrt{s_{NN}} = 200$ GeV for the most central (0–20%) collisions to the recent parton saturation calculation [11] and to the predictions of AMPT model [12]. (b) Same as (a), but for the most peripheral (80–100%) collisions. Gray bands correspond to systematic data errors.

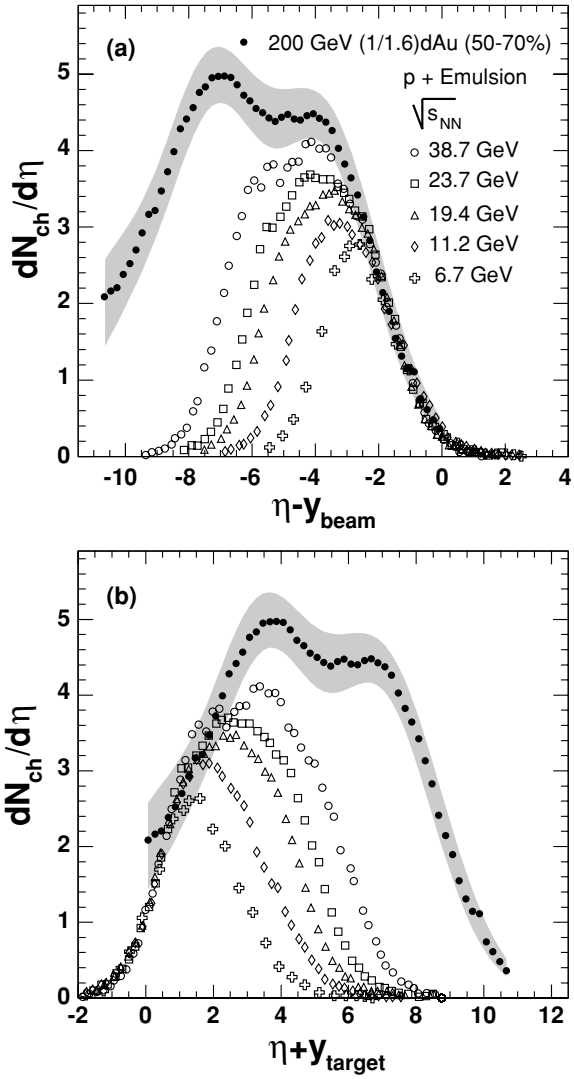

FIG. 6. (a) Comparison of $dN_{\rm ch}/d\eta$ distributions for d+Au collisions scaled (see text) to p+Em collisions (sum of shower and gray tracks) at five energies [4,27,28]. η measured in the c.m. system has been shifted to $\eta - y_{\rm beam}$ to study fragmentation regions in the deuteron/proton rest frame. (b) Same as (a), but shifted to $\eta + y_{\rm target}$ to study fragmentation regions in the gold/Emulsion rest frame.

the deuteron and gold directions. In Ref. [29], we reported a similar comparison but for more central d+Au and p+Pb [3] collisions. This extended longitudinal scaling, also seen earlier in $p(\bar{p})$+p [2], p+A [27,30], and A+A [8] collisions, suggests that the dominance of the two scaling regions is a common longitudinal feature of all multiparticle production processes.

In summary, we find that the longitudinal features of d+Au collisions at $\sqrt{s_{NN}} = 200$ GeV, as reflected by the centrality dependence of the pseudorapidity distributions of charged particles, are very similar to those seen in p+A collisions at energies lower by more than an order of magnitude. In particular, we find that in d+Au collisions, the total multiplicity of charged particles scales linearly with the total number of participants, that the transition between the multiplicity per

participant in d+Au and Au+Au collisions is not controlled simply by the total number of participants, and that the energy dependence of the density of charged particles produced in the fragmentation regions exhibits extended longitudinal scaling. The results can be accommodated in the framework of current models; however, they do impose significant constraint on the models.

This work was partially supported by U.S. DOE Grants DE-AC02-98CH10886, DE-FG02-93ER40802, DE-FC02-94ER40818, DE-FG02-94ER40865, DE-FG02-99ER41099, and W-31-109-ENG-38; U.S. NSF Grants 9603486, 0072204, and 0245011; Polish KBN Grant 1-P03B-062-27 (2004–2007); and NSC of Taiwan Contract NSC 89-2112-M-008-024.

[1] N. N. Nikolaev, Sov. J. Part. Nucl. **12**, 63 (1981); D. Horn, Phys. Rep. **4**, 1 (1972) and references therein.
[2] J. Whitmore, Phys. Rep. **27**, 187 (1976); G. J. Alner *et al*., Z. Phys. C **33**, 1 (1986) and references therein.
[3] W. Busza, Acta Phys. Pol. B **8**, 333 (1977).
[4] S. Fredriksson *et al*., Phys. Rep. **144**, 187 (1987).
[5] H. R. Schmidt *et al*., J. Phys. G. **19**, 1705 (1993).
[6] B. B. Back *et al*., Phys. Rev. Lett. **88**, 022302 (2002).
[7] B. B. Back *et al*., Preprint nucl-ex/0301017, submitted to PRC-RC.
[8] B. B. Back *et al*., Phys. Rev. Lett. **91**, 052303 (2003).
[9] B. B. Back *et al*., Phys. Rev. Lett. **93**, 082301 (2004).
[10] A. Białas and W. Czyz, Acta. Phys. Pol. **B36**, 905 (2005).
[11] D. Kharzeev, E. Levin, and M. Nardi, Nucl. Phys. **A730**, 448 (2004).
[12] Z. W. Lin, S. Pal, C. M. Ko, B. A. Li, and B. Zhang, Nucl. Phys. **A698**, 375 (2004).
[13] B. B. Back *et al*., Nucl. Instrum. Methods A **499**, 603 (2003).
[14] M. Gyulassy and X. N. Wang, Comput. Phys. Commun. **83**, 307 (1994).
[15] Z. W. Lin and C. M. Ko, Phys. Rev. C **68**, 054904 (2003).
[16] R. Brun *et al*., GEANT 3.21, CERN Lib., W5013, 1994.
[17] I. Arsene *et al*., Phys. Rev. Lett. **94**, 032301 (2005).
[18] B. B. Back *et al*., Phys. Rev. Lett. **87**, 102303 (2001).
[19] G. J. Alner *et al*., Z. Phys. C **33**, 1 (1986).
[20] J. E. Elias *et al*., Phys. Rev. D **22**, 13 (1980).
[21] C. DeMarzo *et al*., Phys. Rev. D **29**, 2476 (1984).
[22] S. J. Brodsky, J. F. Gunion, and J. H. Kuhn, Phys. Rev. Lett. **39**, 1120 (1977).
[23] G. J. Alner *et al*., Phys. Rep. **154**, 247 (1987); H. Heiselberg, *ibid.* **351**, 161 (2001).
[24] G. J. Alner *et al*., Phys. Lett. **B167**, 476 (1986).
[25] W. Busza *et al*., Phys. Rev. Lett. **34**, 836 (1975).
[26] A. Białas *et al*., Nucl. Phys. **B111**, 461 (1976).
[27] I. Otterlund *et al*., Nucl. Phys. **B142**, 445 (1978).
[28] A. Abduzhamilov *et al*., Phys. Rev. D **35**, 3537(R) (1987).
[29] R. Nouicer (PHOBOS Collaboration), J. Phys. G: Nucl. Part. Phys. **30**, S1133 (2004).
[30] C. Halliwell *et al*., Phys. Rev. Lett. **39**, 1499 (1977).